

Scaffold function of long noncoding RNA *HOTAIR* in protein ubiquitination

Je-Hyun Yoon^{1,*}, Kotb Abdelmohsen¹, Jiyoung Kim¹, Xiaoling Yang¹, Jennifer L. Martindale¹, Kumiko Tominaga-Yamanaka¹, Elizabeth J. White², Arturo V. Ojalo³, John L. Rinn⁴, Stefan G. Kreft⁵, Gerald M. Wilson², and Myriam Gorospe¹

¹Laboratory of Genetics, National Institute on Aging-Intramural Research Program, NIH, Baltimore, MD 21224, USA;

²Department of Biochemistry and Molecular Biology and Marlene and Stewart Greenebaum Cancer Center, University of Maryland School of Medicine, Baltimore, MD 21201, USA;

³Biosearch Technologies, Inc., Novato, CA 94949, USA;

⁴Department of Stem Cell and Regenerative Biology, Harvard University, Cambridge, MA 02138, USA

⁵Department of Biology, University of Konstanz, 78457 Konstanz, Germany

*Correspondence:

LG, NIA-IRP, NIH

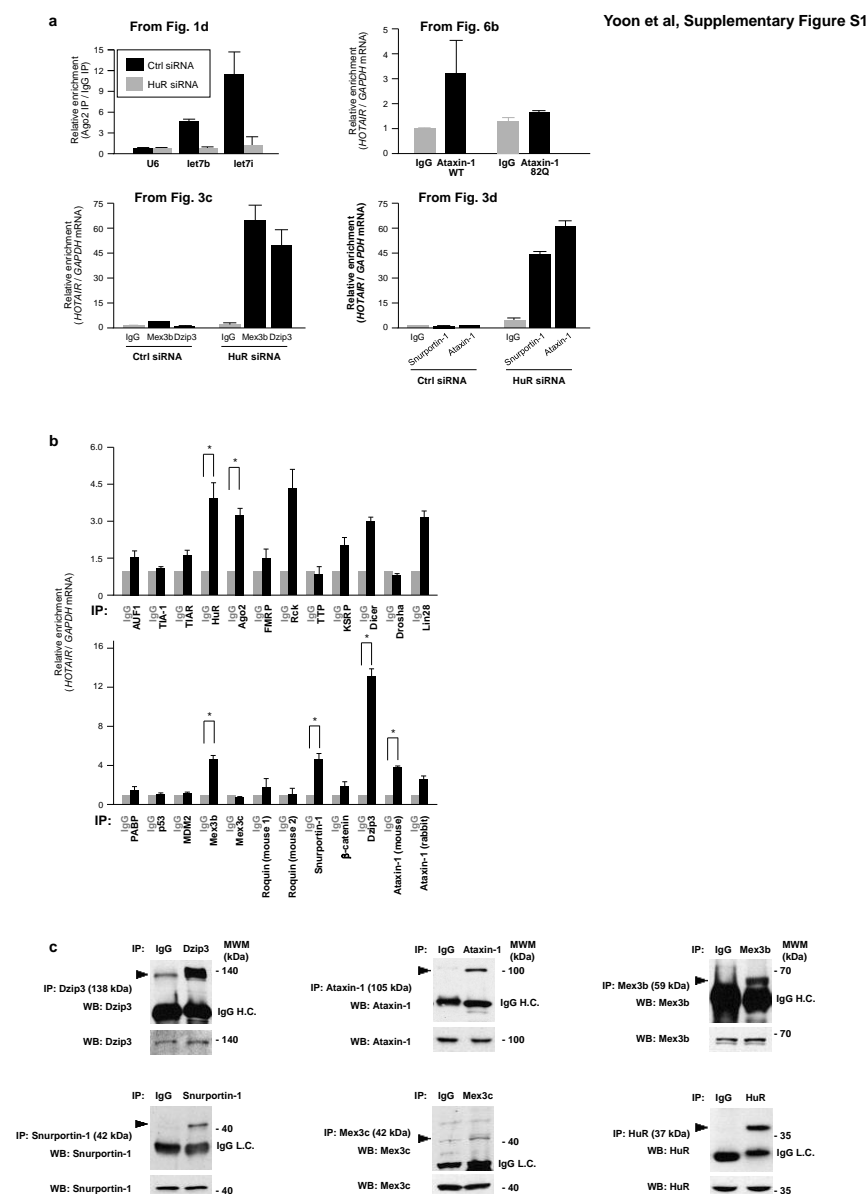
251 Bayview Blvd.

Baltimore, MD 21224, USA

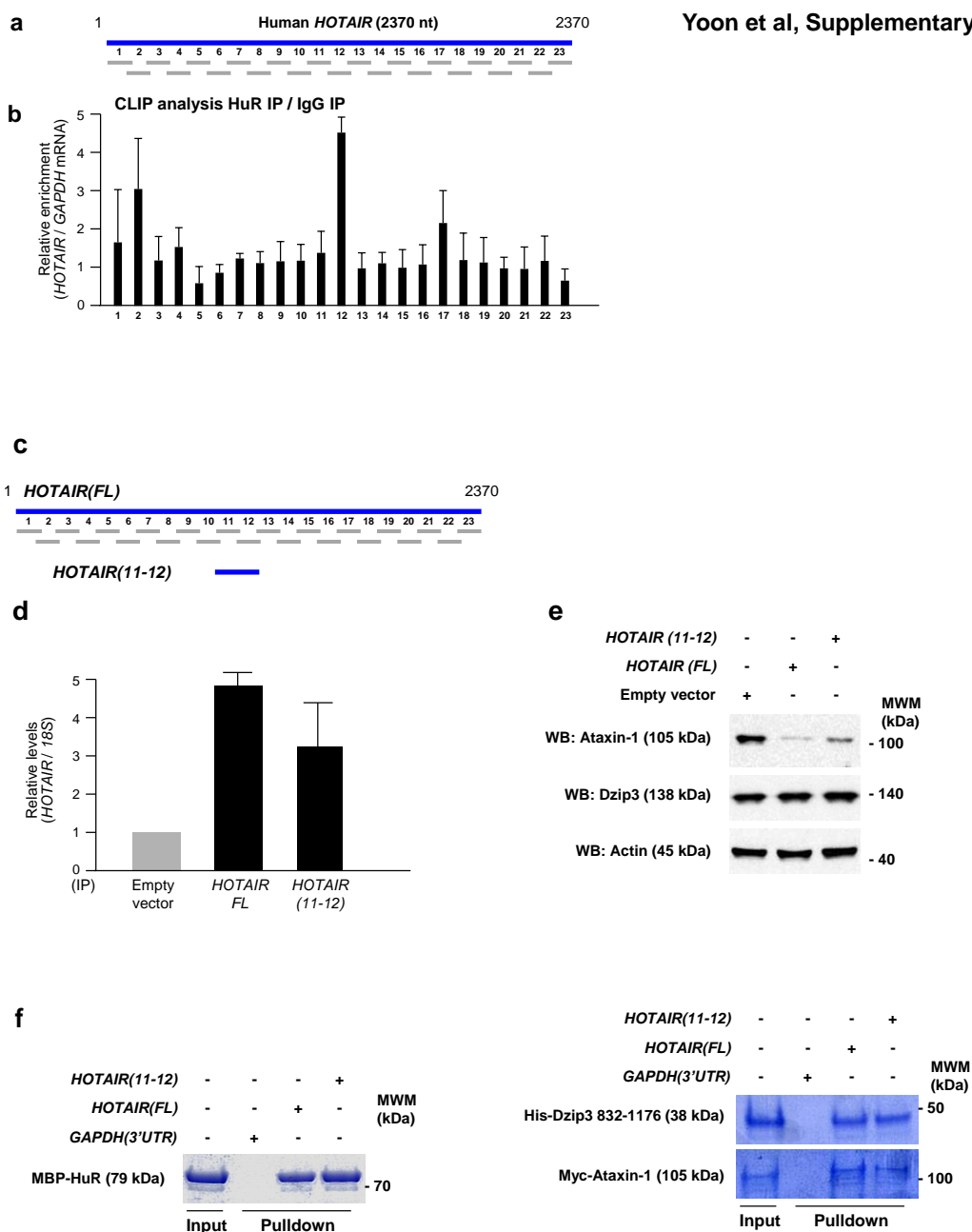
Tel: 410-558-8590 (JHY); Fax: 410-558-8386

yoonyehyun@gmail.com

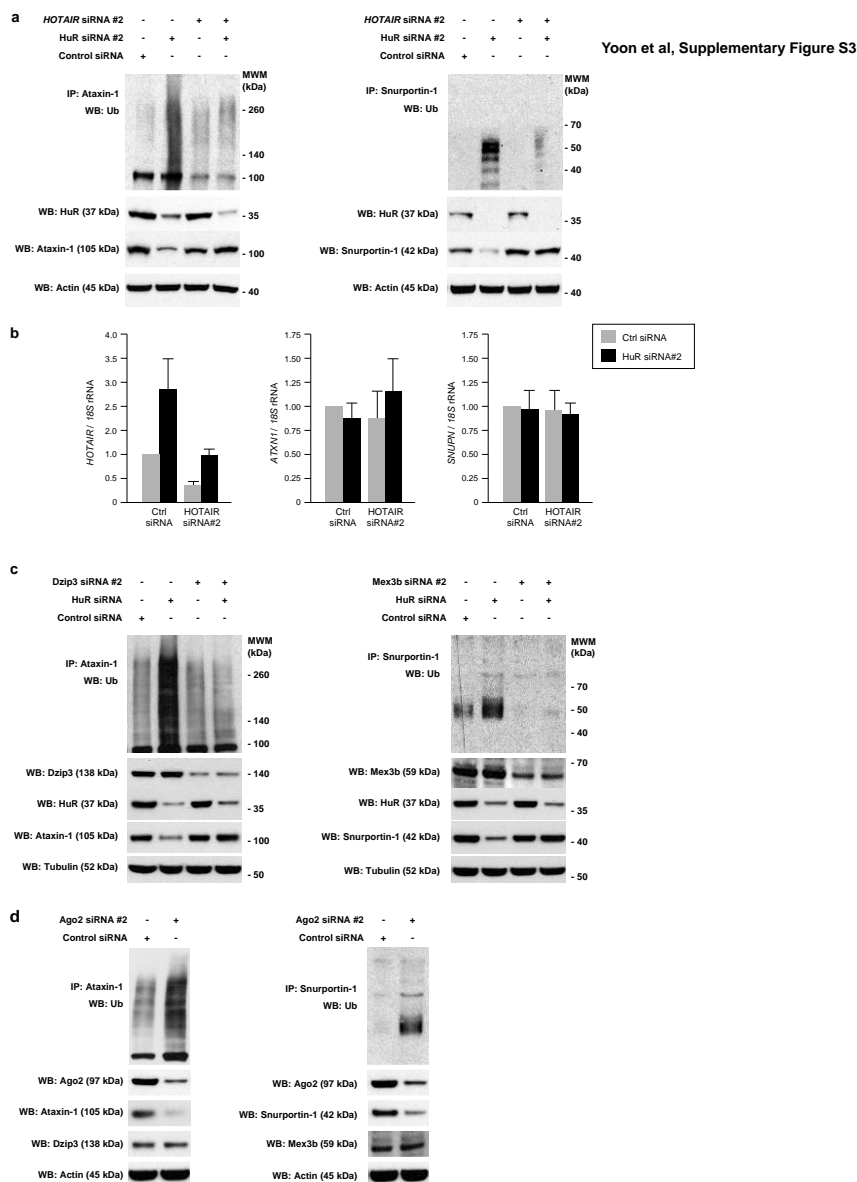
SUPPLEMENTARY FIGURES



Supplementary Figure S1. Survey of RNA-binding proteins associated with *HOTAIR* and IP control assays. (a) Alternative manner of representing RIP assays used in the main article, where the RNA enrichments in the IgG samples are not set as 1.0 but are set relative to the IgG in the respective control group. The graphs represent the means and S.D. from 3 independent experiments. (b) RIP analysis of the interaction of *HOTAIR* with a panel of RBPs in HeLa cell lysates. Antibodies recognizing the RBPs shown were used for IP in each case; control IP reactions were carried out using a corresponding IgG. *HOTAIR* levels were measured by RT-qPCR and normalized to the levels of *GAPDH* mRNA levels in the same IP samples measured by RT-qPCR analysis. Data were quantified as enrichment of *HOTAIR* in the RBP IP relative to the IgG IP. The graphs represent the means and S.D. from 3 independent experiments. *, $P < 0.05$ using Student's *t*-test. (c) Using HeLa cell lysates, the quality of the IP reactions was assayed by Western blot (WB) analysis of Dzip3, Ataxin-1, Mex3b, Mex3c, HuR, and Snurportin-1. Lysates were tested by WB analysis before (lower images for each protein tested) and after IP (top panels for each protein tested). IgG H.C., immunoglobulin heavy chain, IgG L.C., immunoglobulin light chain. Larger fields of blots are shown in Supplementary Figure S7.

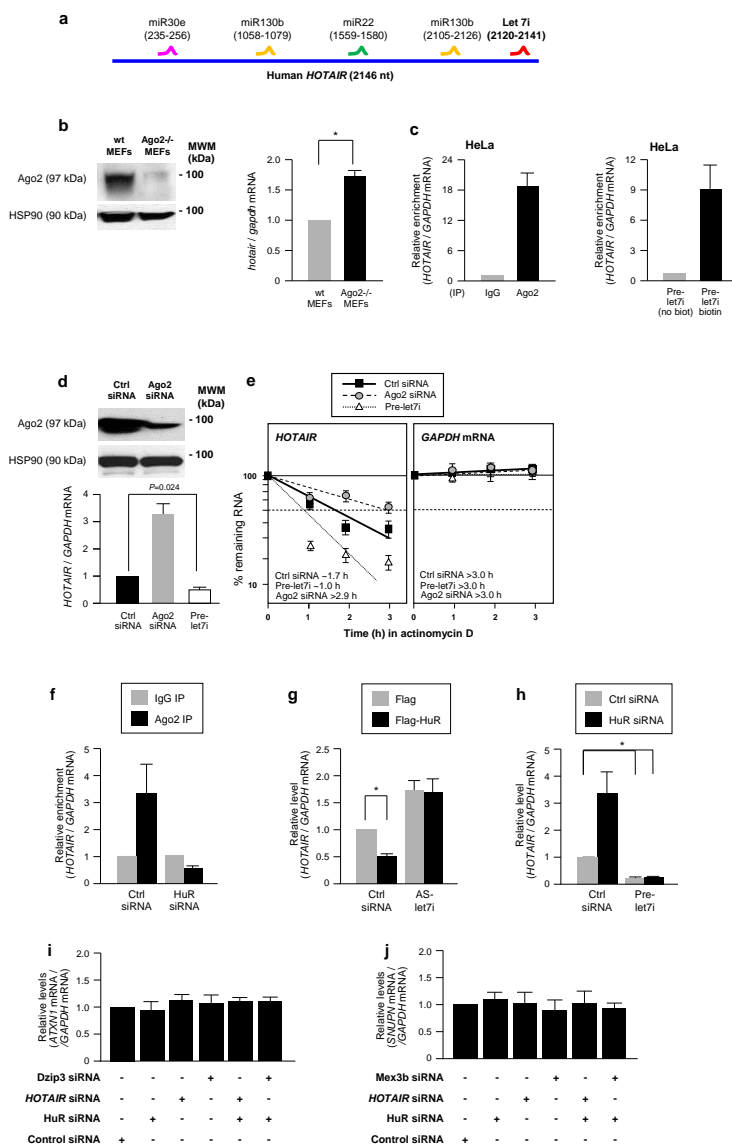


Supplementary Figure S2. Additional characterization of the interaction of *HOTAIR* with HuR, Dzip3, and Ataxin-1. (a,b) Schematic of *HOTAIR* (a) and the segments tested by CLIP analysis (b) following the procedure described in the Methods section, using 10 μ g antibody and 15 mg of crosslinked lysate. (c) A plasmid expressing only segments 11 and 12 of *HOTAIR* (spanning nucleotide positions ~1028-1272, short blue line) was constructed and expressed in HeLa cells. (d,e) Forty-eight hours after transfecting HeLa cells with plasmids to express full-length [*HOTAIR(FL)*] or partial *HOTAIR* [*HOTAIR(11-12)*], as assessed by RT-qPCR (d), the levels of endogenous Ataxin-1, Dzip3, and Actin were determined by Western blot analysis (e). (f) Biotin pulldown analysis to determine the interaction of MBP-HuR (left) or His-Dzip3 (RNA binding domain) or Myc-Ataxin-1 (right) with biotinylated *HOTAIR(FL)*, *HOTAIR(11-12)* or control *GAPDH(3'UTR)*. In (b,d), the graphs reflect the means and S.D. from 3 independent experiments. Larger fields of blots are shown in Supplementary Figure S7.

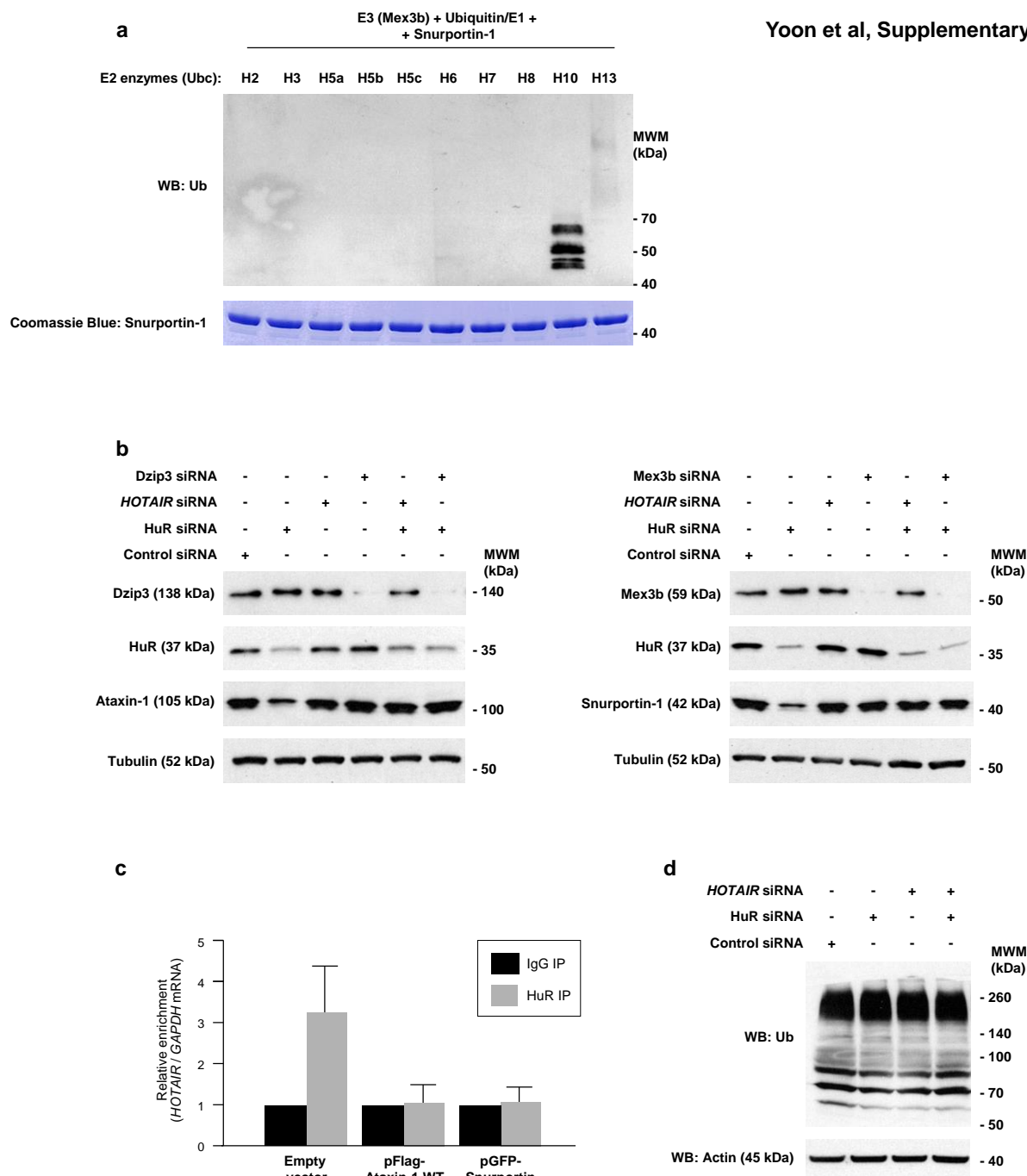


Supplementary Figure S3. Effects of additional *HOTAIR*- or HuR-directed siRNAs. (a) Forty-eight h after silencing HuR with siRNA#2 (Methods), the levels of HuR, Ataxin-1, Snurportin-1, and loading control Actin were assessed by Western blot analysis; the levels of ubiquitinated Ataxin-1, and ubiquitinated Snurportin-1, were assessed by IP of Ataxin-1 or Snurportin followed by ubiquitin Western blot analysis. (b) Forty-eight h after silencing *HOTAIR* with siRNA#2 (Methods) in the presence of either Ctrl siRNA or HuR siRNA#2, the levels of *HOTAIR*, *ATXN1* mRNA, and *SNUPN* mRNA relative to *18S* rRNA were assessed by RT-qPCR analysis. Data are the means and S.D. from 3 independent experiments. (c) Forty-eight h after silencing Dzip3 or Mex3b with siRNA#2 (Methods), the levels of HuR, Dzip3, Mex3b, Ataxin-1, Snurportin-1, and loading control Tubulin were assessed by Western blot analysis; the levels of ubiquitinated Ataxin-1, and ubiquitinated Snurportin-1, were assessed by IP of Ataxin-1 or Snurportin-1 followed by ubiquitin Western blot analysis. (d) Forty-eight h after silencing Ago2 with siRNA#2, the levels of Ago2, Dzip3, Mex3b, Ataxin-1, Snurportin-1, and loading control Actin were assessed by Western blot analysis; the levels of ubiquitinated Ataxin-1, and ubiquitinated Snurportin-1, were assessed by IP of Ataxin-1 or Snurportin followed by ubiquitin Western blot analysis. Larger fields of blots are shown in Supplementary Figure S7.

Yoon et al, Supplementary Figure S4

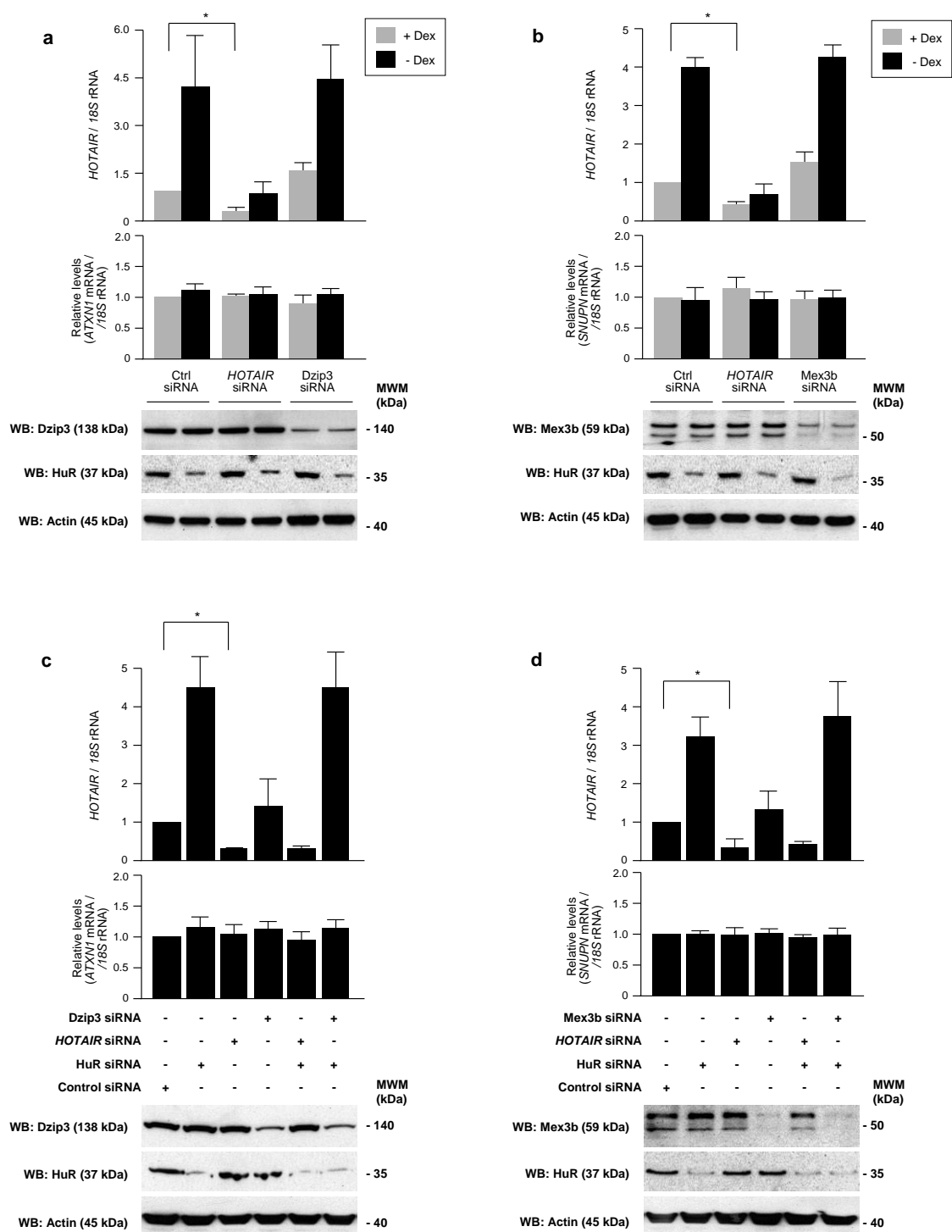


Supplementary Figure S4. HuR and let7i/Ago2 cooperate in promoting *HOTAIR* decay. (a) *HOTAIR* sequence with predicted miRNA target sites. (b) In mouse embryonic fibroblasts (MEFs) isolated from Ago2 knockout mice (Ago2^{-/-}) or wild type mice (wt), Ago2 and control HSP90 levels were assessed by Western blot analysis (left), and *HOTAIR* levels associated with Ago2 were assessed by RIP analysis followed by RT-qPCR (right). (c) Left, RIP analysis of Ago2-bound *HOTAIR* in HeLa cells. Right, 48 h after transfection of HeLa cells with let7i or biotin let7i, the relative enrichment of endogenous *HOTAIR* in biotin pulldown samples (isolated using streptavidin beads) was assessed by RT-qPCR quantitation of *HOTAIR*. (d,e) Forty-eight hours after silencing Ago2 or overexpressing pre-let7i in HeLa cells (d), the steady state levels and half-life of *HOTAIR* and control *GAPDH* mRNA were assessed as explained in Figure 2f (e). (f) Forty-eight hours after transfecting HeLa cells with HuR siRNA, the association of *HOTAIR* with Ago2 was assessed by RIP and RT-qPCR analysis. (g,h) Forty-eight hours after overexpressing Flag-HuR, silencing HuR, overexpressing let7i or expressing a let7i antagomir (AS-let7i), *HOTAIR* abundance was assessed by RT-qPCR. (i,j) The relative abundance of *HOTAIR*, *ATXN1*, *SNUPN* mRNA, and *GAPDH* mRNA in cells processed as shown in Fig. 4e,f was assessed by RT-qPCR analysis. In (b-j), the graphs reflect the means and S.D. from 3 independent experiments. *, $P < 0.05$ using Student's *t*-test. Larger fields of blots are shown in Supplementary Figure S7.



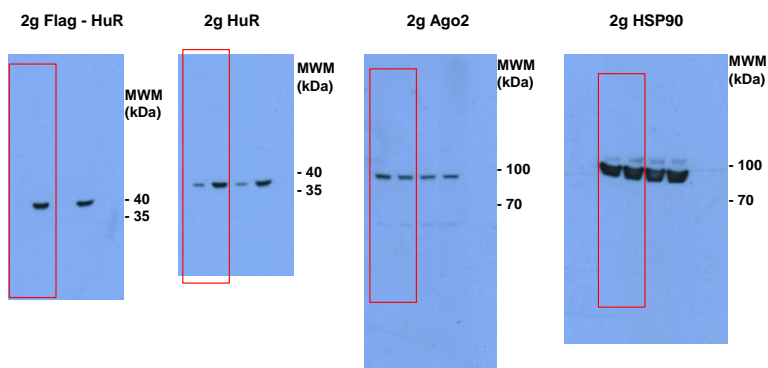
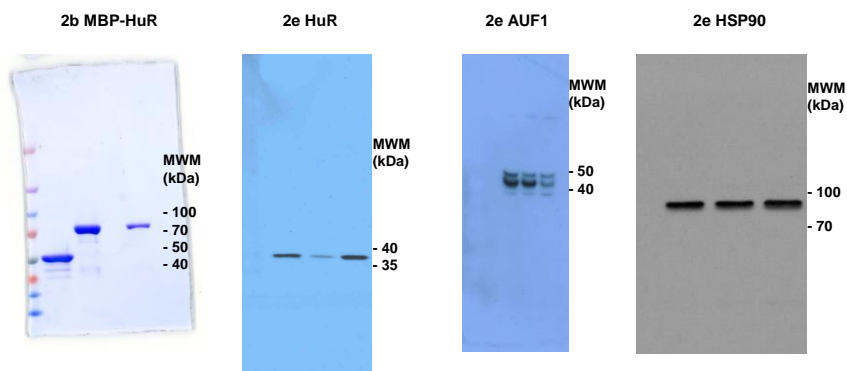
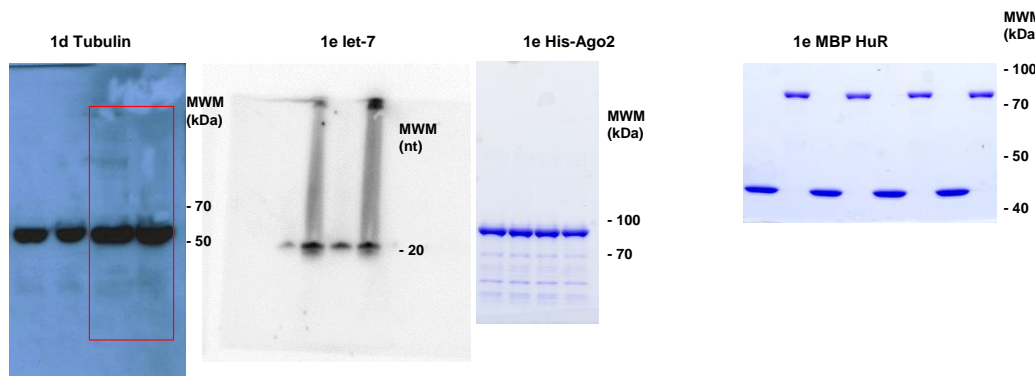
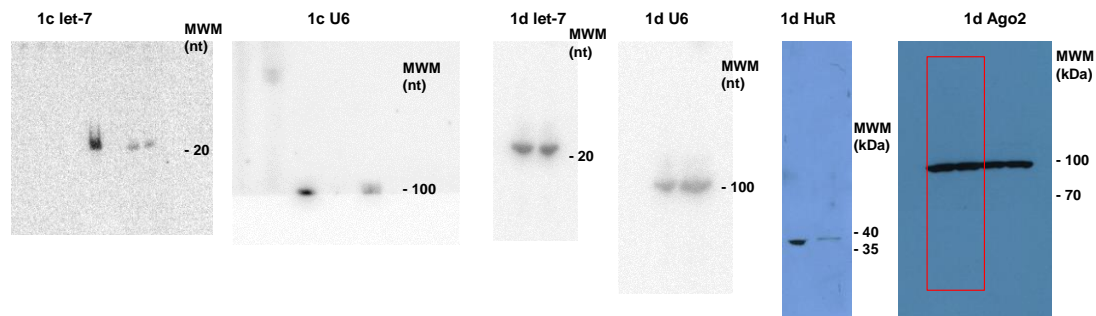
Supplementary Figure S5. Survey of Ubiquitin conjugating (Ubc) E2 enzymes for Snurportin-1, and analysis of silencing results. (a) Various E2 Ubc enzymes were assayed for their effect on ubiquitination of Snurportin-1 *in vitro* following the same procedure as that described in the main Fig. 5b. (b) Western blot analysis of the efficiency of silencing HuR, Dzip3, and Mex3b in HeLa cells used to measure the half-lives of Ataxin-1 and Snurportin-1. (c) Relative enrichment of *HOTAIR* compared to *GAPDH* mRNA from HuR IP after overexpression of empty vector, Flag-Ataxin-1 WT, or GFP-Snurportin. Data are the means and S.D. from 3 independent experiments. (d) Western blot analysis to detect ubiquitinated proteins in cell lysates after silencing HuR and/or *HOTAIR*. Larger fields of blots are shown in Supplementary Figure S7.

Yoon et al, Supplementary Figure S6

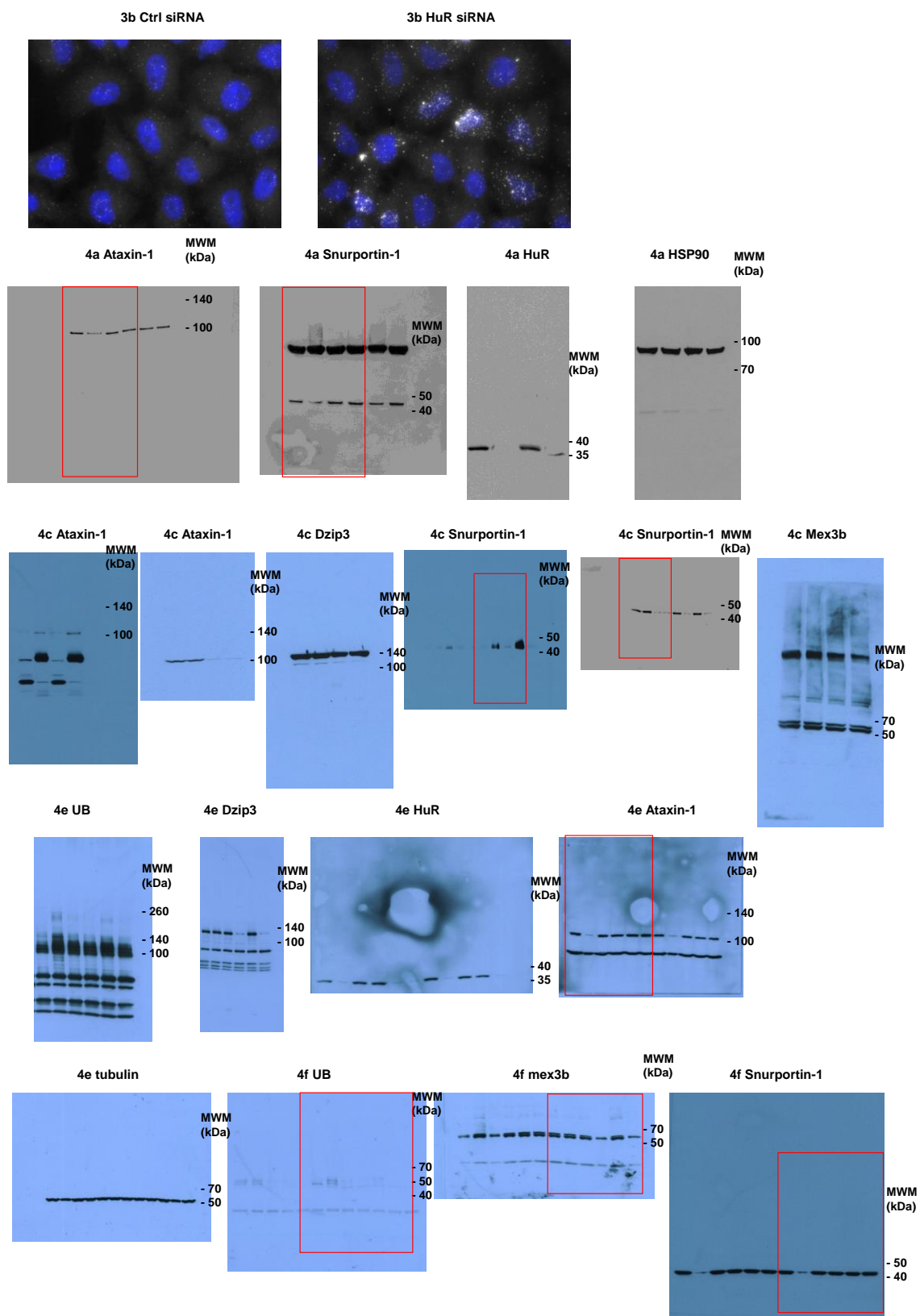


Supplementary Figure S6. RNA expression in IDH4 cells. (a,b) IDH4 cells [proliferating (+Dex) or senescent (-Dex)] were transfected as described in Fig. 6e; 5 days later, the levels of *HOTAIR*, *18S* rRNA, *ATXN1* mRNA (a) and *SNUPN* mRNA (b) were quantified and plotted. (c,d) Proliferating IDH4 cells were transfected as in Fig. 8; 48 h later, the levels of *HOTAIR*, *18S* rRNA, *ATXN1* mRNA (c) and *SNUPN* mRNA (d). In (a-d) the graphs reflect the means and S.D. from 3 independent experiments. *, $P < 0.05$ using Student's *t*-test. Larger fields of blots are shown in Supplementary Figure S7.

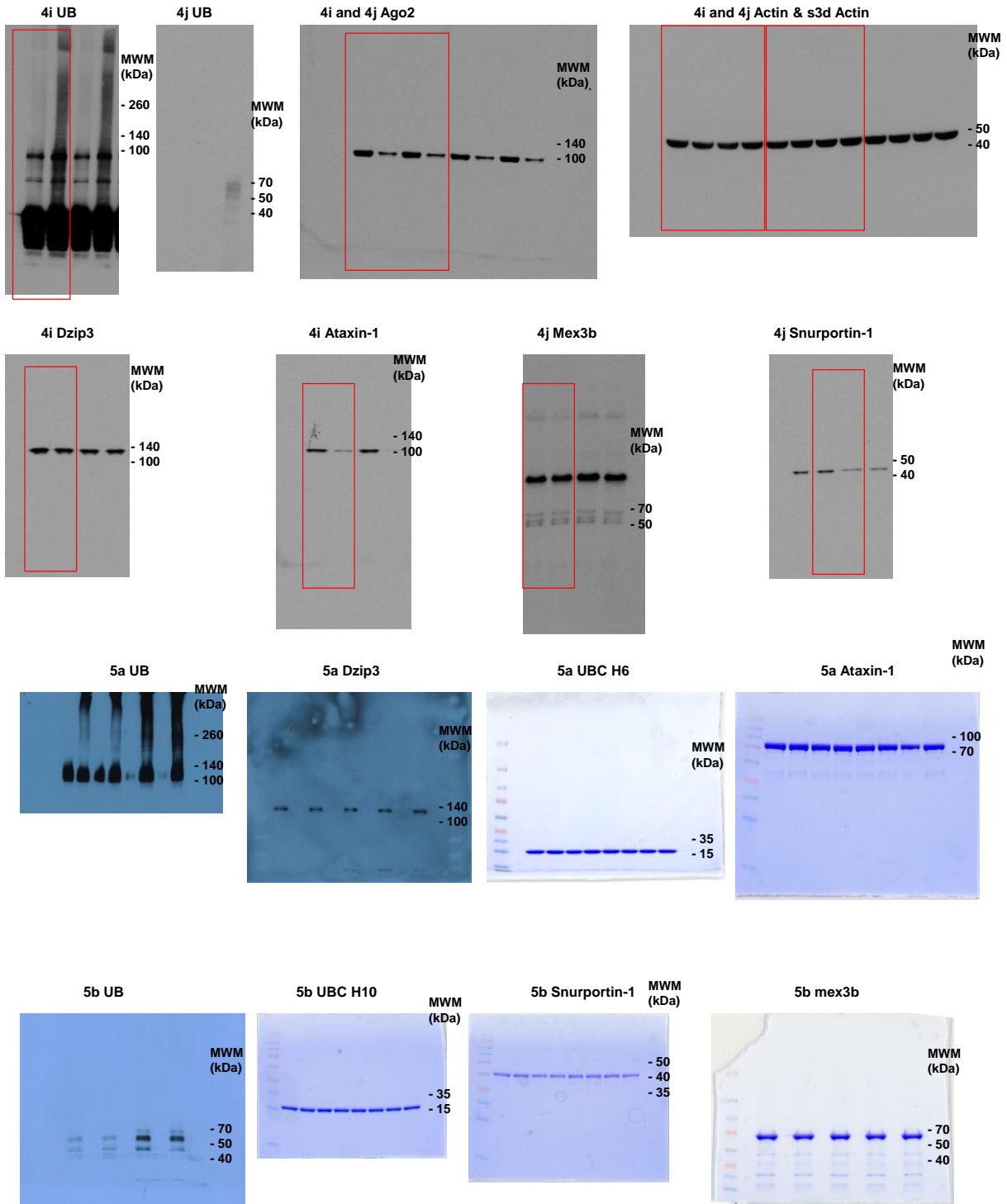
Yoon et al, Supplementary Figure S7



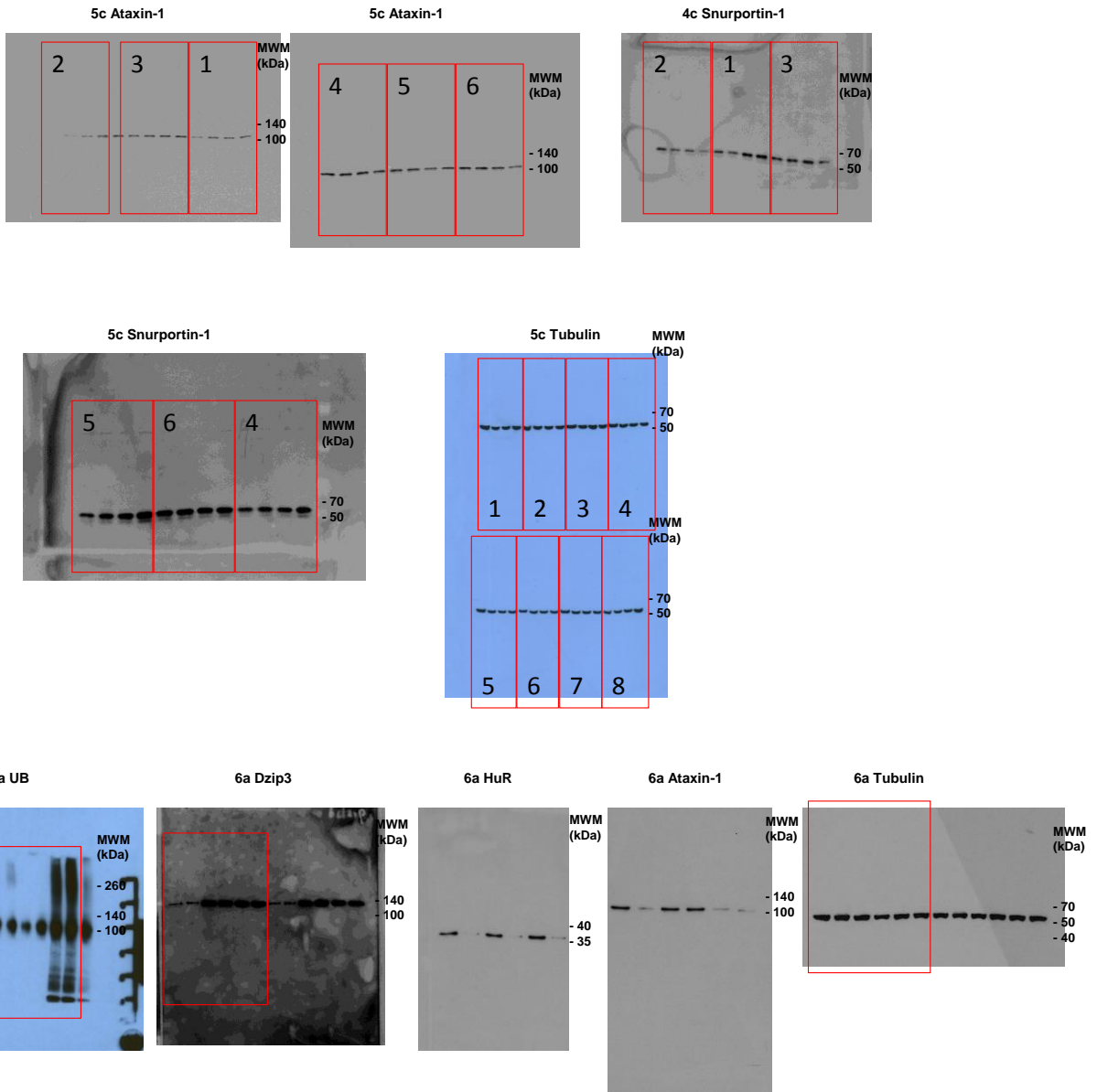
Yoon et al, Supplementary Figure S7



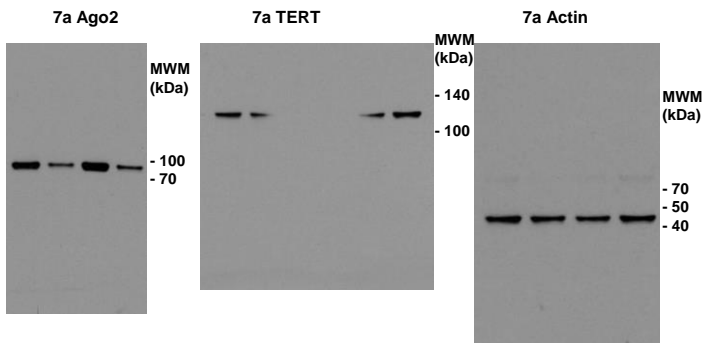
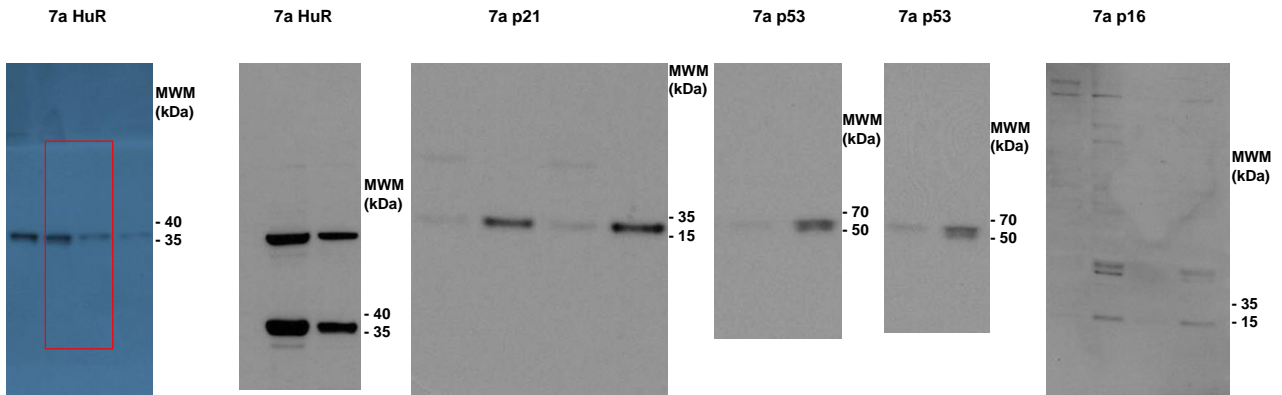
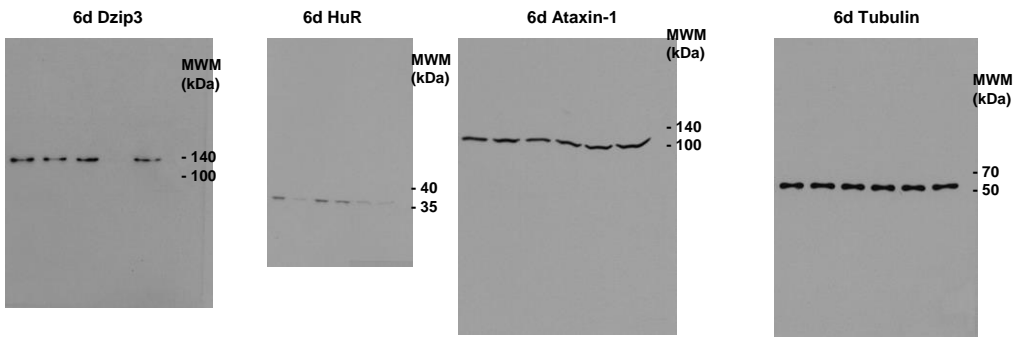
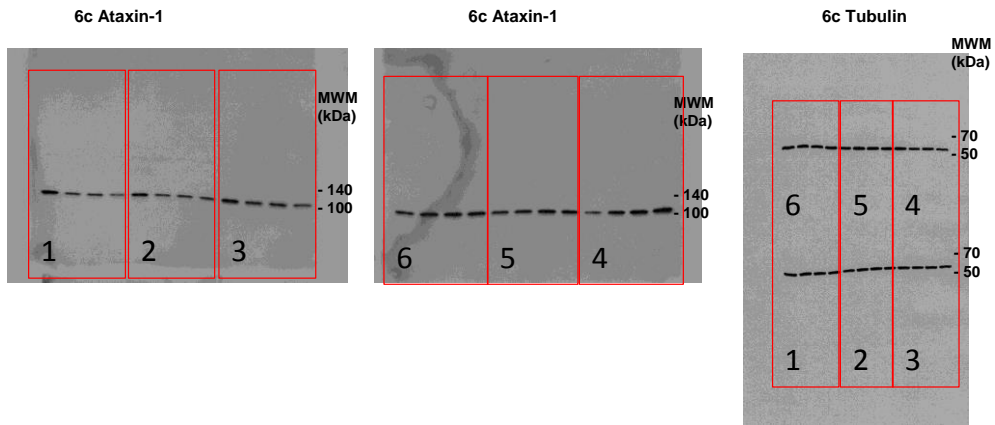
Yoon et al, Supplementary Figure S7



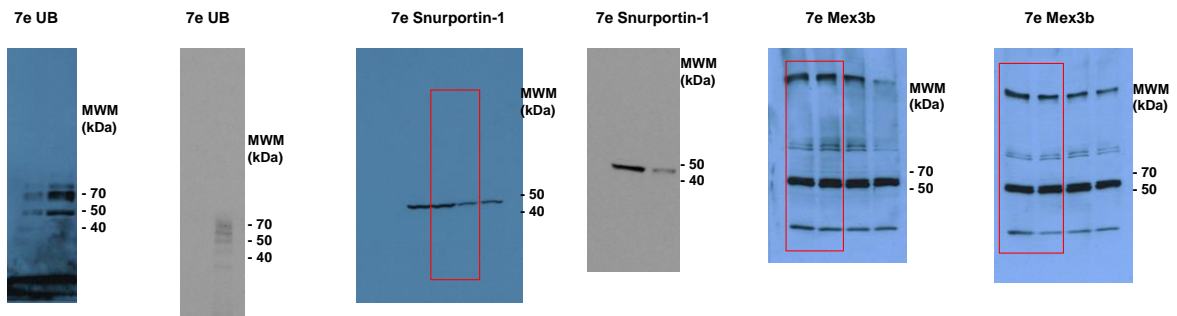
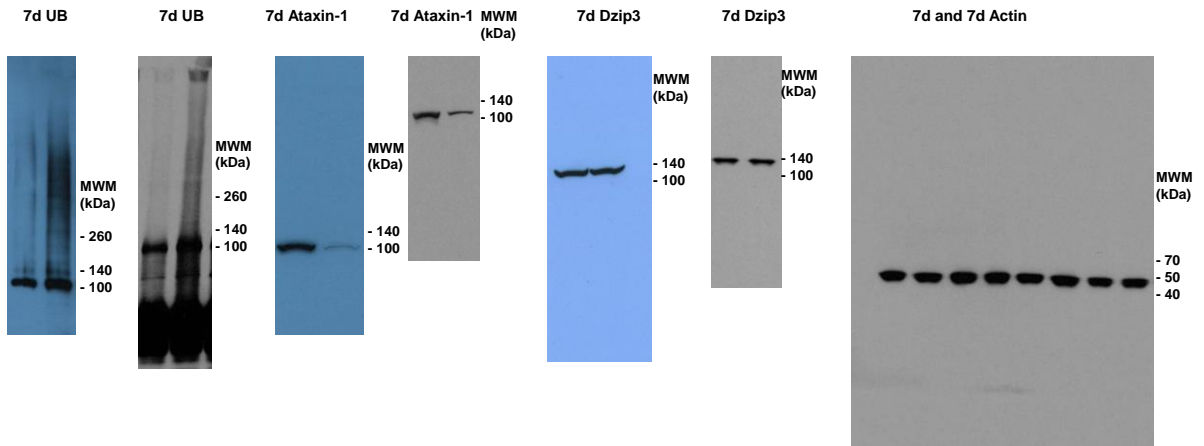
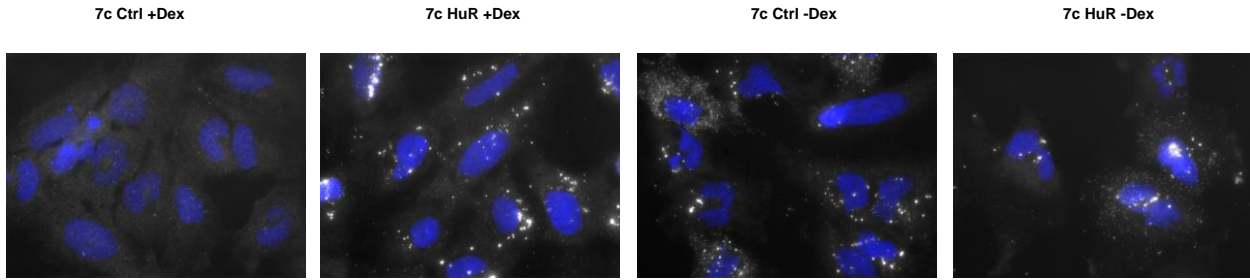
Yoon et al, Supplementary Figure S7



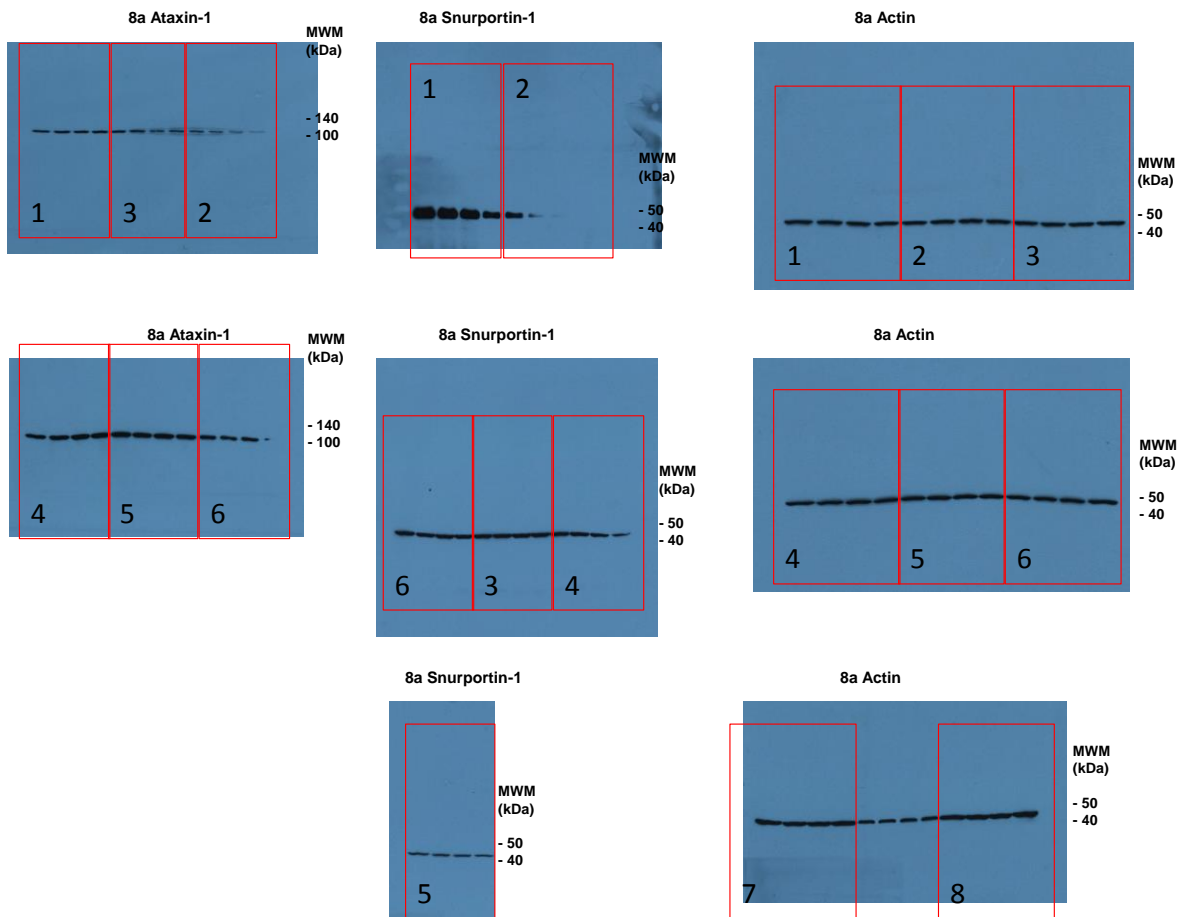
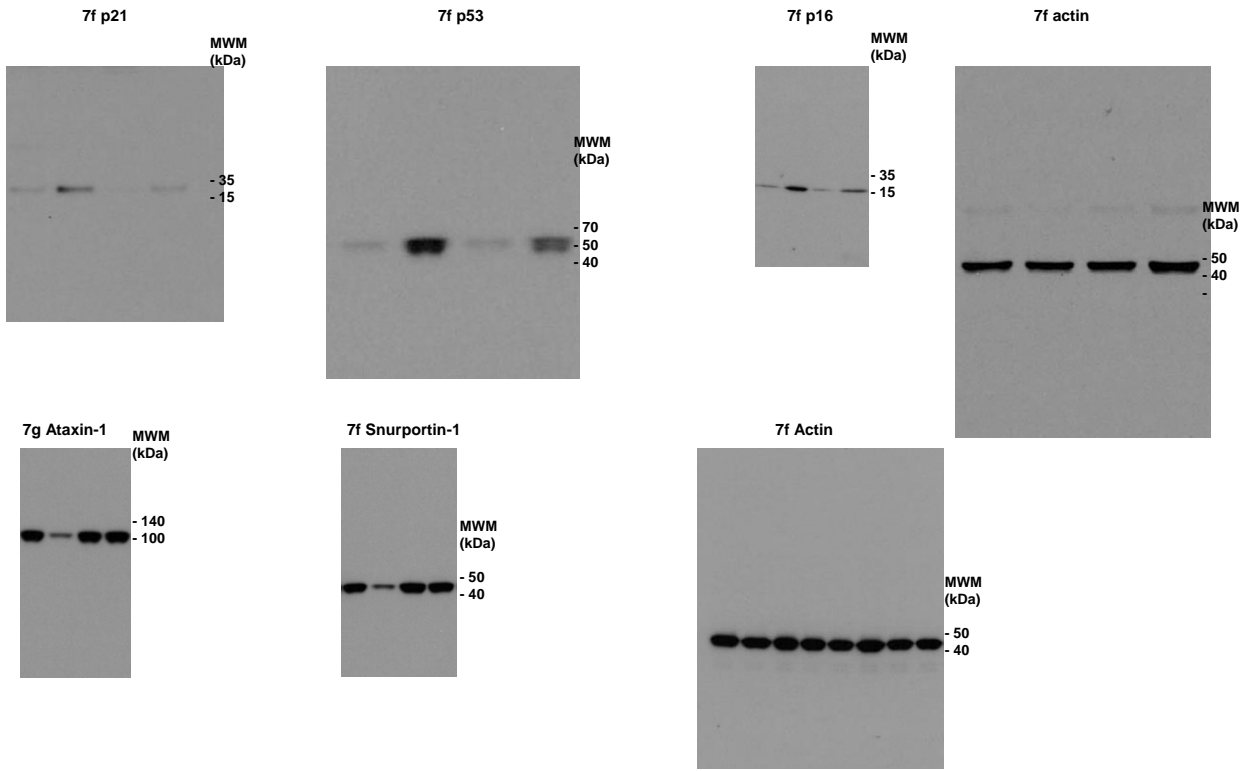
Yoon et al, Supplementary Figure S7



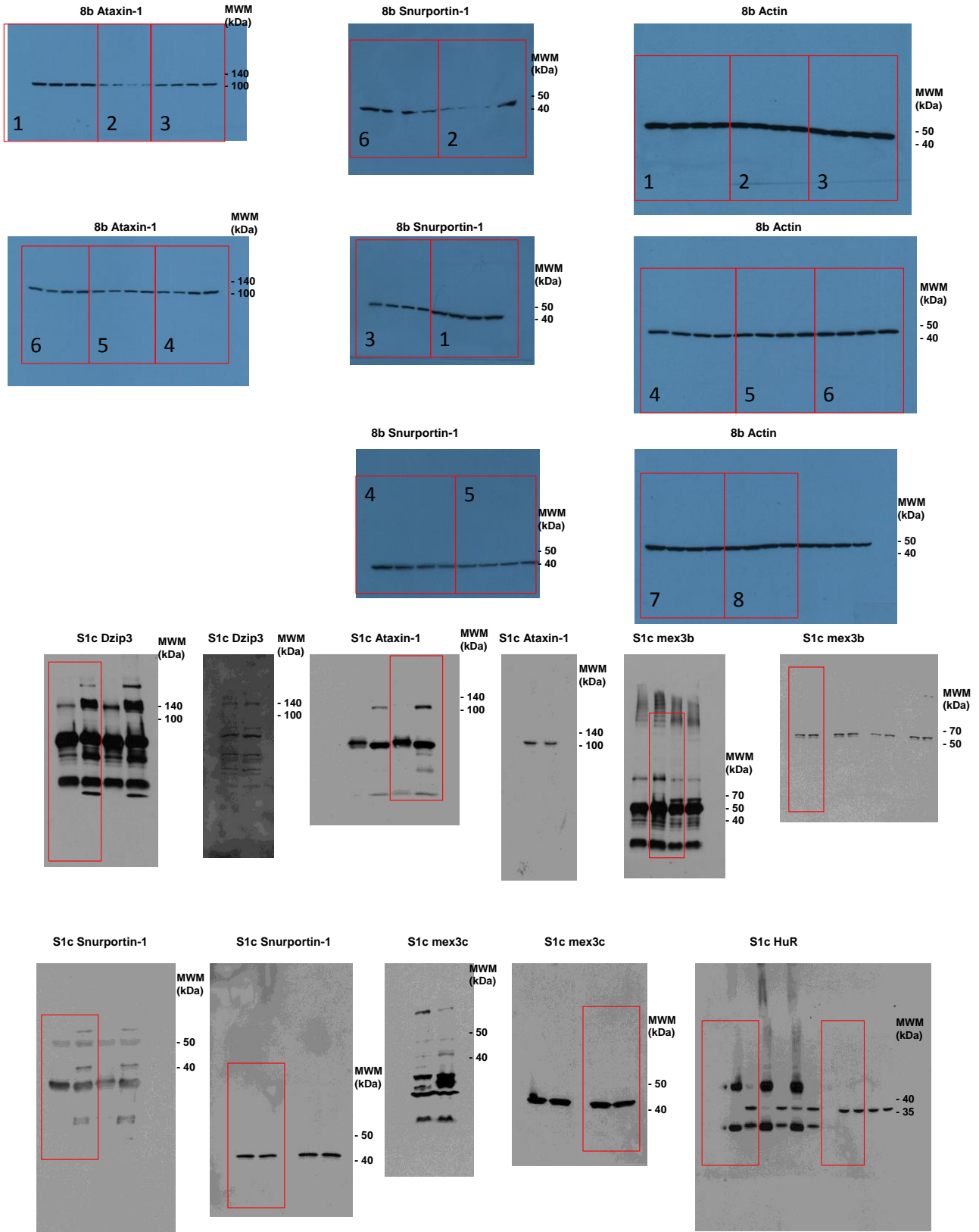
Yoon et al, Supplementary Figure S7



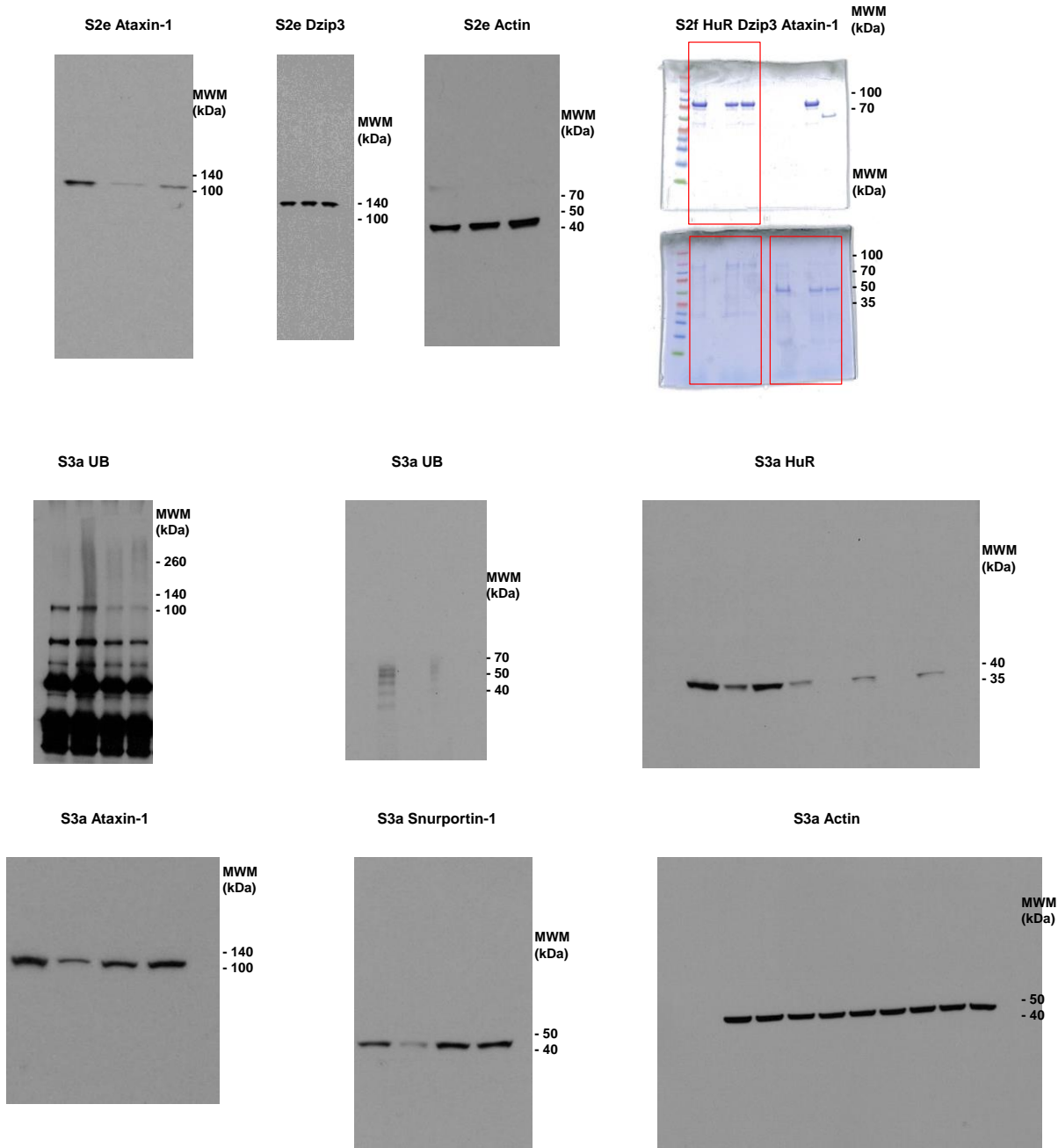
Yoon et al, Supplementary Figure S7



Yoon et al, Supplementary Figure S7



Yoon et al, Supplementary Figure S7



Supplementary Figure S7. Larger fields of blots shown in the Figures 1-9 and Supplementary Figures S1-S6. Larger fields of the blots depicted in the main figures are indicated. The corresponding figure and panel, as well as the molecules (proteins or nucleic acids) detected are indicated above each blot. MWM, molecular weight markers [kDa (kilodaltons) or nt (nucleotides)] are indicated. In blots in which only select lanes were used, red rectangles highlight such lanes.

Name	Species	Sequence	Notes
HOTAIR F	human	GGGGCTTCCTTGCTCTTCTTATC	
HOTAIR R	human	GGTAGAAAAAGCAACCAGGAAGC	
GAPDH F	human	AGCCACATCGCTCAGACAC	
GAPDH R	human	GCCCAATACGACCAAAATCC	
mouse hotair F	mouse	TGATATGGCTGCACGAACA	
mouse hotair R	mouse	TCCTGTTCTTGGCATCTCTG	
mouse gapdh F	mouse	GGGAAATCAACGGCACAGT	
mouse gapdh R	mouse	AGATGGTGATGGGCTTCCC	
let7b	human	TGAGGTAGTAGTTGTGTGGTT	
let7i	human	TGAGGTAGTAGTTGTGTGGTT	
U6 F	human	CGCTTCGGCAGCACATATAC	
U6 R	human	AAAAATGGAACGCTTCAACGA	
ATXN1 F	human	TCGGTGGAGCTTGGTTTACAA	
ATXN1 R	human	GGGAGGACCCAAATGAAGTGG	
SNUPN F	human	CAAGCGGCTGGATTATGTGAA	
SNUPN R	human	AGGAACGTCAATTAACCACTCAG	
18S rRNA F	human	CGAACGCTGCGCCATCAACTT	
18S rRNA R	human	ACCCGTGGTCCACATGGTA	
let7 Northern blot	human	AACCACACAACCTACTACCTCA	
U6 Northern blot	human	AAAAATGGAACGCTTCAACGA	
GAPDH 3'UTR F	human	CCAAGTCTTAATACGACTCACTATAGGGAGA CCTCAACGACCCTTTGTCA	
GAPDH 3'UTR R	human	GGTTGACACAGGGTACTTTTAT	
HOTAIR 1001 F	human	AAAAGGATCC TGAGGCTTGTAAACAAGACCAG	
HOTAIR 1200 R	human	AAAAGCGGCGCTTGAGAGACAGTGCACTCACGC	
			HOTAIR
			fragments amplified
HOTAIR segment 1F	human	GACAGGGTCTGGACAGAAG	27-144
HOTAIR segment 1R	human	GAGTCAGAGTCCCACTGC	
HOTAIR segment 2F	human	GCAGTGGGGAACCTCGACTC	125-250
HOTAIR segment 2R	human	GGGTGTTGCTCTGGAACT	
HOTAIR segment 3F	human	AGAGAGCACAGGCACTGAG	223-380
HOTAIR segment 3R	human	TCCCCTACTGCAGGCTTCTA	
HOTAIR segment 4F	human	CAGTGGAAATGGAAACGATTT	342-471
HOTAIR segment 4R	human	TCAGACTCTTTGGGCGCTTA	
HOTAIR segment 5F	human	AAGGCCCAAGAGTCTGAT	453-581
HOTAIR segment 5R	human	CAGGTCCGTAAGGCTTAGG	
HOTAIR segment 6F	human	CTGGCAGAGAAAAGGCTGAA	505-628
HOTAIR segment 6R	human	CTCCCTCCTCTGGCTCTCT	
HOTAIR segment 7F	human	AGCCAGAGGAGGGAAGAGAG	613-800
HOTAIR segment 7R	human	TTTTCCCTTTCTCATGGA	
HOTAIR segment 8F	human	GGGCACTCACAGACAGAGGT	725-881
HOTAIR segment 8R	human	TCAGGTTTTCCAGCGTCT	
HOTAIR segment 9F	human	AGAACGCTGGAAAAACCTGA	862-991
HOTAIR segment 9R	human	TGGAGATGATAAGGAAGCAAGG	
HOTAIR segment 10F	human	GTCAGCCACTGCCCCACAC	910-1031
HOTAIR segment 10R	human	GCCAGCTCTCTGGCTTTGT	
HOTAIR segment 11F	human	TGGCCAAAGCACTCTATCTC	1028-1143
HOTAIR segment 11R	human	GTGTAGACGCCCATATTT	
HOTAIR segment 12F	human	ACGGAAACCCATGGACTCATA	1142-1272
HOTAIR segment 12R	human	TGGTCCCATTTGGATCTTTC	
HOTAIR segment 13F	human	CAAATGTCAGAGGTTCTGGGA	1217-1324
HOTAIR segment 13R	human	TTGGGGAAGCATTTTCTGAC	
HOTAIR segment 14F	human	TGGGAGTGTGTTTGTGGGA	1331-1441
HOTAIR segment 14R	human	CTACACAAACCCCTTCGCTTC	
HOTAIR segment 15F	human	GAAGCGAAGGGGTTGTAG	1422-1596
HOTAIR segment 15R	human	AGGCTAGGGCTGGTTTCACT	
HOTAIR segment 16F	human	CCCTAGCCTTTGGAAGCTCT	1588-1700
HOTAIR segment 16R	human	TGCTCTGTGCTGCCAGTTAG	
HOTAIR segment 17F	human	AGGAATCCACCTGCCTGTTA	1628-1755
HOTAIR segment 17R	human	ACCCATGTGTCTCAAGATGC	
HOTAIR segment 18F	human	AATGCATCTTGAGACACATGG	1733-1833
HOTAIR segment 18R	human	AGAGTGCAAAAGTCCCGTTTG	
HOTAIR segment 19F	human	CAAACGGGACTTTGCACTCT	1814-1925
HOTAIR segment 19R	human	CCCTTCTGTGTCTACATGC	
HOTAIR segment 20F	human	GCATGTAGACACAGAAGGGGTA	1906-2005
HOTAIR segment 20R	human	CAGGCATTGGGAATGTGTAAT	
HOTAIR segment 21F	human	GCCTGAACCTCCTCTGCTA	2001-2157
HOTAIR segment 21R	human	TGCATACCTACCAATGTATGG	
HOTAIR segment 22F	human	TTCCATACATTGGTAGGTATGC	2134-2236
HOTAIR segment 22R	human	GCACAGAAAATGCATCCAGA	
HOTAIR segment 23F	human	TCTGGATGATTTTCTGTGC	2217-2331
HOTAIR segment 23R	human	ACCACACACACACAACCC	

Supplementary Table S1. DNA primers used in this study.